

Noise-induced switching between vortex states with different polarization in classical two-dimensional easy-plane magnets

Yuri Gaididei

Institute for Theoretical Physics, 252143 Kiev, Ukraine

Till Kampeter and Franz G. Mertens

Physikalisches Institut, Universität Bayreuth, D-95440 Bayreuth, Germany

Alan Bishop

Theoretical Division and Center for Nonlinear Studies, Los Alamos National Laboratory, Los Alamos, New Mexico 87545, USA

In the 2-dimensional anisotropic classical Heisenberg model with XY -symmetry there are nonplanar vortices which exhibit a localized structure of the z -components of the spins around the vortex center. We study how thermal noise induces a transition of this structure from one polarization to the opposite one. We describe the vortex core by a discrete Hamiltonian and consider a stationary solution of the Fokker-Planck equation. We find a bimodal distribution function and calculate the transition rate using Langer's instanton theory (1969). The result is compared with Langevin dynamics simulations for the full many-spin model.

PACS: 05.40.+j, 75.10.Hk, 02.50.Ey, 75.30.Gw

I. INTRODUCTION

There are several classes of quasi-2D (two-dimensional) magnetic materials for which the ratio of inter- to intra-plane magnetic coupling constants is typically $10^{-3} - 10^{-6}$: (1) Layered magnets [1,2,3,4], like K_2CuF_4 , Rb_2CrCl_4 , $(\text{CH}_3\text{NH}_3)_2\text{CuCl}_4$, and $\text{BaM}_2(\text{XO}_4)$ with $\text{M}=\text{Co}, \text{Ni}, \dots$ and $\text{X}=\text{As}, \text{P}, \dots$ (2) CoCl_2 graphite intercalation compounds [5], (3) magnetic lipid layers, like manganese stearate [6]. Many of these materials can be described by the classical 2D Heisenberg model with XY - or "easy-plane" symmetry (section II).

In this model vortices play the decisive role: they are responsible for a topological phase transition [7,8] at the Kosterlitz-Thouless temperature T_c and, above T_c , for "central peaks" in the dynamic form factors for the spin correlations. The central peaks were observed in inelastic neutron scattering experiments [9,10,11,12,13] and in combined Monte Carlo/Spin Dynamics simulations [14,15,16,17,18,19]. The observed central peaks agree qualitatively, partially even quantitatively, with the central peaks which were obtained by a vortex-gas approach [14,15,16,17,18,19].

There are two types of static vortex solutions whose structure and energy differ, depending on the anisotropy of the Heisenberg exchange interaction [16]. For strong anisotropy (i. e., if the anisotropy parameter δ exceeds a threshold δ_c) only planar vortices are stable for which all spins are lying in the easy plane (xy -plane). For weak anisotropy ($0 < \delta < \delta_c$) only nonplanar vortices are stable, which exhibit a localized structure of the z -components of the spins around the vortex center. In addition to the vorticity $q = \pm 1, \pm 2, \dots$, the nonplanar vortices have a second topological charge p . It is denoted "polarization" because its sign determines the side of the xy -plane to which the out-of-plane vortex structure points. The planar vortices can be considered as having $p = 0$.

The product qp of the topological charges determines the dynamics because the vortices are subject to a "gyrocoupling force" $\vec{G} \times \vec{V}$, which is formally equivalent to the Lorentz force [20,21]: \vec{V} is the velocity of the vortex center, but instead of an external magnetic field we have here an intrinsic quantity, produced by the vortex itself and carried along with it: The "gyrovector" $\vec{G} = 2\pi qp\vec{e}_z$ which is orthogonal to the xy -plane. The formula for \vec{G} was derived in the continuum limit and, strictly speaking, \vec{G} is conserved only in this limit. Nevertheless, spin dynamics simulations for 1 or 2 vortices showed that the direction of \vec{G} (or the sign of p , because q is always conserved) does not change during the simulation [22,23].

However, we know so far three exceptions, i. e. situations in which the out-of-plane vortex structure can suddenly make a transition from one polarization to the opposite one. As the direction of \vec{G} is reversed, this has a drastic effect on the dynamics: The direction of the gyrocoupling force is also reversed, which means that the direction of the vortex motion is reversed, too. The three transition mechanisms are:

(1) Interaction with spin waves. The easiest way to see this is to use "dirty" initial conditions for the spin dynamics simulation [24]: E. g., a structure which is not a good approximation to the 1-vortex solution (this solution can be obtained numerically by an iteration procedure [24]). Then many spin waves are radiated at the beginning of the simulation, while the approximate vortex structure adapts to the lattice and becomes a "good" solution (numerically identical to the above solution obtained by iterations). The emitted spin waves form a magnon gas; i. e. the vortex moves in a kind of magnon thermostat and transitions to the opposite polarization occur with a certain probability which depends on how dirty the initial condition was.

(2) An ac magnetic field. If the amplitude of a field which rotates in the easy plane is larger than a threshold value, a transition to the opposite polarization occurs. In contrast to (1), the reverse process does not occur because the field breaks the symmetry of the two polarizations. This will be the subject of a forthcoming paper.

(3) Thermal noise. This has some similarity with (1), although that is a deterministic zero-temperature effect. In section II we implement white noise into the microscopic equations (the Landau-Lifshitz eq.) by adding stochastic magnetic fields to the local fields in which every spin precesses. In this way we model the interactions of the spin degrees of freedom with thermostat degrees of freedom (magnons, phonons etc.). We consider a stationary solution \mathcal{P}_{st} of the Fokker-Planck equation, using a reduced Hamiltonian which models the vortex core. Such a core Hamiltonian was used in [25,26] for the calculation of δ_c . For a certain parameter range, \mathcal{P}_{st} exhibits two maxima (for the two possible polarizations of a nonplanar vortex) and a saddle point (corresponding to the planar vortex).

In section III we calculate the probability flux over the region around the saddle point using Langer's instanton theory [27]. Here we use the fact that for $\delta \rightarrow \delta_c$ there is a soft mode among the normal modes which were obtained numerically for a system with one vortex [28].

Finally, our prediction for the transition rate is tested by Langevin dynamics simulations, i. e. by integration of the stochastic Landau-Lifshitz equation. For these tests the design of the simulations, including the choice of the parameter ranges, turns out to be decisive.

II. HAMILTONIAN AND THE FOKKER-PLANCK EQUATION

We consider a Heisenberg model with XY- or easy-plane symmetry with classical spins $\vec{S}_{\vec{n}}$ located on the sites $\vec{n} = (n_x, n_y)$ of a square lattice

$$H = - \sum_{\vec{n}, \vec{\Delta}} J_{\vec{\Delta}} \left(S_{\vec{n}}^x S_{\vec{n}-\vec{\Delta}}^x + S_{\vec{n}}^y S_{\vec{n}-\vec{\Delta}}^y + \lambda S_{\vec{n}}^z S_{\vec{n}-\vec{\Delta}}^z \right) \quad (1)$$

where λ is the anisotropy parameter ($0 \leq \lambda < 1$), $J_{\vec{\Delta}} \equiv J$ is the exchange integral and $\vec{\Delta} = (\Delta_x, \Delta_y)$ is a vector which connects a spin with its nearest neighbors ($\Delta_x = \pm 1, \Delta_y = 0$ or $\Delta_y = \pm 1, \Delta_x = 0$). The spin dynamics is governed by the Landau-Lifshitz equation. Since we want to study the interaction with thermal noise, we implement a noise and a damping term

$$\frac{d}{dt} \vec{S}_{\vec{n}} = -\vec{S}_{\vec{n}} \times \left(\frac{\partial H}{\partial \vec{S}_{\vec{n}}} + \vec{h}_{\vec{n}}(t) \right) + \gamma \vec{S}_{\vec{n}} \times \left(\vec{S}_{\vec{n}} \times \frac{\partial H}{\partial \vec{S}_{\vec{n}}} \right) \quad (2)$$

Here we have added a stochastic magnetic field $\vec{h}_{\vec{n}}(t)$ to the local field $\frac{\partial H}{\partial \vec{S}_{\vec{n}}}$ in which the spin $\vec{S}_{\vec{n}}$ precesses. Since $\vec{h}_{\vec{n}}$ is multiplied with $\vec{S}_{\vec{n}}$, this means multiplicative noise.

Another way to obtain the stochastic term in Eq. (2) consists in adding to the Hamiltonian interactions between the spins and local stochastic magnetic fields

$$V(t) = - \sum_{\vec{n}} \vec{h}_{\vec{n}}(t) \vec{S}_{\vec{n}}. \quad (3)$$

We use Gaussian white noise with

$$\begin{aligned} \langle h_{\vec{n}}^\alpha(t) \rangle &= 0, \\ \langle h_{\vec{n}}^\alpha(t) h_{\vec{n}'}^{\alpha'}(t') \rangle &= 2 D_\alpha \delta_{\vec{n}\vec{n}'} \delta_{\alpha\alpha'} \delta(t-t'), \end{aligned} \quad (4)$$

where D_α is the variance of the noise. In order to preserve the isotropy in the easy plane we demand

$$D_x = D_y \equiv D. \quad (5)$$

The last term in Eq. (2) represents damping in the Landau-Lifshitz form (see [7]). An alternative would be the Gilbert damping which yields the same results, however, as we will use only very small damping coefficients.

It is convenient to use a representation for the classical spin vector $\vec{S}_{\vec{n}}$ in terms of two angles of rotation $\theta_{\vec{n}}$ and $\Phi_{\vec{n}}$

$$\vec{S}_{\vec{n}} = S \{ \sin \theta_{\vec{n}} \cos \Phi_{\vec{n}}, \sin \theta_{\vec{n}} \sin \Phi_{\vec{n}}, \cos \theta_{\vec{n}} \} \quad (6)$$

The variables $M_{\vec{n}} = \cos \theta_{\vec{n}}$ and $\Phi_{\vec{n}}$ constitute a pair of canonically conjugated variables, which means that in the no-damping case ($\gamma = 0$)

$$\begin{aligned} \frac{d\Phi_{\vec{n}}}{dt} &= \frac{\partial(H+V)}{\partial M_{\vec{n}}}, \\ \frac{dM_{\vec{n}}}{dt} &= -\frac{\partial(H+V)}{\partial \Phi_{\vec{n}}}. \end{aligned} \quad (7)$$

Here

$$\begin{aligned} H &= -J \sum_{\vec{n}, \vec{\Delta}} \left(\lambda M_{\vec{n}} M_{\vec{n}-\vec{\Delta}} + P_{\vec{n}} P_{\vec{n}-\vec{\Delta}} \cos(\Phi_{\vec{n}} - \Phi_{\vec{n}-\vec{\Delta}}) \right) \\ V(t) &= - \sum_{\vec{n}} \left(h_{\vec{n}}^z(t) M_{\vec{n}} + P_{\vec{n}} (h_{\vec{n}}^x(t) \cos(\Phi_{\vec{n}}) + h_{\vec{n}}^y(t) \sin(\Phi_{\vec{n}})) \right) \end{aligned} \quad (8)$$

is the Hamiltonian of the system in terms of the new variables and $P_{\vec{n}} = \sqrt{1 - M_{\vec{n}}^2}$.

Using the variables $M_{\vec{n}}$ and $\Phi_{\vec{n}}$ the Landau-Lifshitz equation (2) can be written as a set of coupled stochastic equations

$$\begin{aligned}
\frac{d\Phi_{\vec{n}}}{dt} &= \frac{\partial H}{\partial M_{\vec{n}}} - \frac{\gamma}{1 - M_{\vec{n}}^2} \frac{\partial H}{\partial \Phi_{\vec{n}}} + f_{\vec{n}}(M_{\vec{n}}, \Phi_{\vec{n}}, t) , \\
\frac{dM_{\vec{n}}}{dt} &= -\frac{\partial H}{\partial \Phi_{\vec{n}}} - \gamma(1 - M_{\vec{n}}^2) \frac{\partial H}{\partial M_{\vec{n}}} + g_{\vec{n}}(M_{\vec{n}}, \Phi_{\vec{n}}, t) .
\end{aligned} \tag{9}$$

where

$$\begin{aligned}
f_{\vec{n}}(M_{\vec{n}}, \Phi_{\vec{n}}, t) &= -h_{\vec{n}}^z(t) + \frac{M_{\vec{n}}}{P_{\vec{n}}} (h_{\vec{n}}^x(t) \cos(\Phi_{\vec{n}}) + h_{\vec{n}}^y(t) \sin(\Phi_{\vec{n}})) , \\
g_{\vec{n}}(M_{\vec{n}}, \Phi_{\vec{n}}, t) &= -P_{\vec{n}} (h_{\vec{n}}^x(t) \sin(\Phi_{\vec{n}}) - h_{\vec{n}}^y(t) \cos(\Phi_{\vec{n}}))
\end{aligned} \tag{10}$$

are multiplicative stochastic forces. From Eqs (4), (5) and (10) we obtain

$$\begin{aligned}
\langle f_{\vec{n}}(M_{\vec{n}}, \Phi_{\vec{n}}, t) f_{\vec{n}'}(M_{\vec{n}'}, \Phi_{\vec{n}'}, t') \rangle &= 2\delta(t - t') \delta_{\vec{n}\vec{n}'} \left(D_z + D \frac{M_{\vec{n}} M_{\vec{n}'}}{P_{\vec{n}} P_{\vec{n}'}} \cos(\Phi_{\vec{n}} - \Phi_{\vec{n}'}) \right) , \\
\langle g_{\vec{n}}(M_{\vec{n}}, \Phi_{\vec{n}}, t) g_{\vec{n}'}(M_{\vec{n}'}, \Phi_{\vec{n}'}, t') \rangle &= 2D\delta(t - t') \delta_{\vec{n}\vec{n}'} P_{\vec{n}} P_{\vec{n}'} \cos(\Phi_{\vec{n}} - \Phi_{\vec{n}'}) \\
\langle f_{\vec{n}}(M_{\vec{n}}, \Phi_{\vec{n}}, t) g_{\vec{n}'}(M_{\vec{n}'}, \Phi_{\vec{n}'}, t') \rangle &= 2D\delta(t - t') \delta_{\vec{n}\vec{n}'} M_{\vec{n}} \frac{P_{\vec{n}'}}{P_{\vec{n}}} \sin(\Phi_{\vec{n}} - \Phi_{\vec{n}'})
\end{aligned} \tag{11}$$

We have introduced the stochastic magnetic fields $\vec{h}_{\vec{n}}(t)$ to model the interaction of the spin degrees of freedom with thermostat degrees of freedom: phonons, electrons, other magnetic excitations etc. However, it is clear that the thermostat excitations are characterized by finite correlation times and a more appropriate modelling of the influence of these excitations would be to use colored noise. The problem under consideration is very complicated, however, if considered in the framework of a nonwhite-noise approach. Therefore we restrict ourselves to the case (4), where we understand the white noise approach as a limiting case of the colored-noise process and therefore we consider Eqs (9), (10) as Stratonovich stochastic differential equations [8].

From Eqs (9)-(11) we obtain that the equation for the probability density function

$$\mathcal{P}(m_{\vec{n}}, \phi_{\vec{n}}, t) = \langle \prod_{\vec{n}} \delta(m_{\vec{n}} - M_{\vec{n}}(t)) \delta(\phi_{\vec{n}} - \Phi_{\vec{n}}(t)) \rangle \tag{12}$$

has the form

$$\begin{aligned}
\frac{\partial}{\partial t} \mathcal{P} &= \sum_{\vec{n}} \frac{\partial}{\partial \phi_{\vec{n}}} \left(\left(-\frac{\partial H}{\partial m_{\vec{n}}} + \frac{\gamma}{1 - m_{\vec{n}}^2} \frac{\partial H}{\partial \phi_{\vec{n}}} \right) \mathcal{P} + \left(D_z + D \frac{m_{\vec{n}}^2}{1 - m_{\vec{n}}^2} \right) \frac{\partial}{\partial \phi_{\vec{n}}} \mathcal{P} \right) - \\
&\sum_{\vec{n}} \frac{\partial}{\partial m_{\vec{n}}} \left(\left(\frac{\partial H}{\partial \phi_{\vec{n}}} + \gamma(1 - m_{\vec{n}}^2) \frac{\partial H}{\partial m_{\vec{n}}} \right) \mathcal{P} + D(1 - m_{\vec{n}}^2) \frac{\partial}{\partial m_{\vec{n}}} \mathcal{P} \right)
\end{aligned} \tag{13}$$

As was mentioned above, the stochastic magnetic fields $\vec{h}_{\vec{n}}(t)$ model the interaction with thermostat degrees of freedom. Therefore it is quite natural to demand that Eq. (13) has a stationary solution in the form of the Gibbs distribution

$$\mathcal{P}_{st} \sim \exp \left(-\frac{H}{T} \right) . \tag{14}$$

It is seen from Eq. (13) that the function (14) is a steady-state solution of the Fokker-Planck equation (13) when the fluctuation-dissipation condition

$$D_z = D = \gamma T \tag{15}$$

is fulfilled. Here T is the temperature of the crystal. Under the condition (15) the Fokker-Planck equation for the function \mathcal{P} has the form

$$\begin{aligned}
\frac{\partial}{\partial t} \mathcal{P} &= \sum_{\vec{n}} \frac{\partial}{\partial \phi_{\vec{n}}} \left(\left(-\frac{\partial H}{\partial m_{\vec{n}}} + \frac{\gamma}{1 - m_{\vec{n}}^2} \frac{\partial H}{\partial \phi_{\vec{n}}} \right) \mathcal{P} + \gamma T \frac{1}{1 - m_{\vec{n}}^2} \frac{\partial}{\partial \phi_{\vec{n}}} \mathcal{P} \right) - \\
&\sum_{\vec{n}} \frac{\partial}{\partial m_{\vec{n}}} \left(\left(\frac{\partial H}{\partial \phi_{\vec{n}}} + \gamma(1 - m_{\vec{n}}^2) \frac{\partial H}{\partial m_{\vec{n}}} \right) \mathcal{P} + \gamma T(1 - m_{\vec{n}}^2) \frac{\partial}{\partial m_{\vec{n}}} \mathcal{P} \right)
\end{aligned} \tag{16}$$

Let us consider first the equilibrium properties of the system. We assume that a vortex is situated in the center of a unit cell at the origin of a coordinate system. The static in-plane vortex ($m_{\vec{n}} = 0$) is characterized by the angles $\Phi_{\vec{n}}^0$ which satisfy the equation

$$\sum_{\vec{\Delta}} \sin(\Phi_{\vec{n}}^0 - \Phi_{\vec{n}-\vec{\Delta}}^0) = 0. \quad (17)$$

The $\Phi_{\vec{n}}^0$ are approximately given by the usual in-plane vortex structure

$$\Phi_{\vec{n}}^0 = q \arctan\left(\frac{n_y}{n_x}\right) \quad (18)$$

where $n_x, n_y = (2n+1)/2, n = 0, \pm 1, \pm 2, \dots$ (the lattice constant is chosen equal to 1) and the integer q is the vorticity. It is known [25], [28] that the in-plane vortex is stable for $0 < \lambda < \lambda_c$ where the critical value λ_c of the anisotropy parameter depends on the type of the lattice (e.g. for square lattices $\lambda_c \simeq 0.703$ [26]). For $\lambda > \lambda_c$ the in-plane vortex becomes unstable and an out-of-plane vortex is created. To gain insight as to how the temperature influences the stability conditions we need a reduced form of the Hamiltonian (8) which effectively takes into account both types of vortices: in-plane and out-of-plane. Such an effective Hamiltonian was proposed in [25]. It was shown in [25] that the dynamics of the vortex instability can be understood under the following assumptions:

- i) The in-plane angles $\Phi_{\vec{n}}^0$ for static in-plane and out-of-plane vortices are given by Eq. (17).
- ii) The deviations $\psi_{\vec{n}} = \Phi_{\vec{n}} - \Phi_{\vec{n}}^0$ of the in-plane angles from their static values are radially symmetric. They strongly decay with the distance $r_{\vec{n}} = \sqrt{(n_x - 1/2)^2 + (n_y - 1/2)^2}$ from the vortex center:

$$\psi_{\vec{n}} = \begin{cases} \psi_1, & \text{for } \vec{n} = \pm(1/2, 1/2), \pm(-1/2, 1/2) \\ \psi_2, & \text{for } \vec{n} = \pm(3/2, 1/2), \pm(-1/2, 3/2) \\ \psi_3, & \text{for } \vec{n} = \pm(1/2, 3/2), \pm(-3/2, 1/2) \\ 0, & \text{otherwise} \end{cases} \quad (19)$$

- iii) The deviations of the out-of-plane components are also radially symmetric and decay strongly

$$m_{\vec{n}} = \begin{cases} m_1, & \text{for } \vec{n} = \pm(1/2, 1/2), \pm(-1/2, 1/2) \\ m_2, & \text{for } \vec{n} = \pm(3/2, 1/2), \pm(-1/2, 3/2) \\ m_3, & \text{for } \vec{n} = \pm(1/2, 3/2), \pm(-3/2, 1/2) \\ 0, & \text{otherwise} \end{cases} \quad (20)$$

Under these assumptions the dynamics of the vortex core is described by the following Hamiltonian

$$\begin{aligned} H_c = & -4J \{ \lambda (m_1^2 + m_1(m_2 + m_3) + m_2 m_3) \\ & + \cos \delta_1 p_1 (p_2 \cos(\psi_1 - \psi_2) + p_3 \cos(\psi_1 - \psi_3)) \\ & + (\cos \delta_1 + \cos \delta_2) (p_2 \cos \psi_2 + p_3 \cos \psi_3) \\ & + p_2 p_3 \sin(2\delta_1) \cos(\psi_2 - \psi_3) \} \end{aligned} \quad (21)$$

with

$$p_\alpha = \sqrt{1 - m_\alpha^2}, \quad \alpha = 1, 2, 3 \quad (22)$$

and

$$\delta_1 = \Phi_{1/2,1/2}^0 - \Phi_{3/2,1/2}^0, \quad \delta_2 = \Phi_{3/2,1/2}^0 - \Phi_{5/2,1/2}^0. \quad (23)$$

Using the approximation $\psi_2 = \psi_3, m_2 = m_3$ and the static in-plane angle distribution (18), we get $\cos \delta_1 = 2/\sqrt{5}, \cos \delta_2 = 8/\sqrt{65}$ and in this case the Hamiltonian (21) coincides with the Hamiltonian in [25].

Being interested in the distribution of the out-of-plane components m_α we integrate the function (14) with respect to the in-plane angles ψ_α . We obtain a reduced stationary probability density

$$\begin{aligned} \mathcal{P}_{st}(m_1, m_2, m_3) = & \frac{1}{\mathcal{N}} e^{\lambda \beta (m_1^2 + m_1(m_2 + m_3) + m_2 m_3)} \\ & \int_0^{2\pi} d\phi e^{\beta \sin(2\delta_1) p_2 p_3 \cos \phi} I_0(\beta \cos \delta_1 p_1 \sqrt{p_2^2 + p_3^2 + 2p_2 p_3 \cos \phi}) \times \\ & I_0(\beta (\cos \delta_1 + \cos \delta_2) \sqrt{p_2^2 + p_3^2 + 2p_2 p_3 \cos \phi}), \end{aligned} \quad (24)$$

where $\beta = 4J/T$ is a dimensionless inverse temperature. \mathcal{N} is the normalization factor and $I_0(x)$ is a modified Bessel function [30,31].

The analysis of the function (24) shows that it has a unique maximum at $m_1 = m_2 = m_3 = 0$ if the anisotropy parameter λ is below a temperature dependent threshold value $\lambda_c(T)$. This case corresponds to the stable in-plane vortex. If

$$\lambda > \lambda_c(T) \quad (25)$$

the function (24) has two maxima at $m_1 = \pm m_1^0, m_2 = \pm m_2^0, m_3 = \pm m_3^0$ and a saddle point at $m_1 = m_2 = m_3 = 0$. In this case the probability density function (24) describes a bistable system of two out-of-plane vortex structures with opposite polarizations.

Let us illustrate this statement by a crude approach when only two degrees of freedom m_1 and ψ_1 are included. In this case the core Hamiltonian (21) simplifies to

$$H_c = -4J\{\lambda m_1^2 + 2\cos\delta_1 p_1 \cos\psi_1\} \quad (26)$$

The corresponding stationary distribution $\mathcal{P}_{st}(m_1, \psi_1)$ is plotted in Fig. 1a (without normalization). The reduced stationary probability density (24) has the form

$$\begin{aligned} \mathcal{P}_{st}(m_1) &= \exp(\beta\lambda m_1^2) I_0(2\beta\cos\delta_1 p_1) / \mathcal{N} , \\ \mathcal{N} &= \int_{-1}^1 dm_1 \exp(\beta\lambda m_1^2) I_0(2\beta\cos\delta_1 p_1) \end{aligned} \quad (27)$$

The function $\mathcal{P}_{st}(m_1)$ describes a bimodal distribution (see Fig.1(b)) in the range

$$\beta\cos^2\delta_1 > \lambda > \cos\delta_1 \frac{I_1(2\beta\cos\delta_1)}{I_0(2\beta\cos\delta_1)} \quad (28)$$

A more accurate approach is based on the expansion of the Hamiltonian (21) into a series with respect to $\{\psi\}$. Then in the harmonic approximation with respect to the ψ_α the stationary probability density is determined by the expression

$$\begin{aligned} \mathcal{P}_{st}(m_1, m_2, m_3) &= \\ \frac{1}{\mathcal{N}} &\frac{\exp(\beta H_c(\{m\}, \{\psi\} = 0))}{\sqrt{p_1 p_2 p_3 (p_2 + p_3) (\sin(2\delta_1) (p_2 + p_3) + p_1 \cos\delta_1 + \cos\delta_1 + \cos\delta_2)}} \end{aligned} \quad (29)$$

The function (29) describes a bimodal distribution if

$$\lambda > \lambda(\beta) \equiv \frac{4\beta\cos\delta_1(2\cos\delta_1 + \cos\delta_2 + 2\sin 2\delta_1) - 2\sin 2\delta_1 - \cos\delta_2 - 3\cos\delta_1}{4\beta(2\sin 2\delta_1 + \cos\delta_2 + 2\cos\delta_1)} . \quad (30)$$

Thus the function (24) has two maxima at $m_1 = \pm m_1^0, m_2 = \pm m_2^0, m_3 = \pm m_3^0$ and a saddle point at $m_1 = m_2 = m_3 = 0$. The phase diagram (the bifurcation curve $\lambda(\beta)$) is shown in Fig. 2. It is worth noting that for a given anisotropy parameter λ the phase which corresponds to the in-plane vortex is always the low-temperature phase.

III. SWITCHING RATE

Following Langer [27] (see also Ref. [29]) it is convenient to introduce a new set of variables $\{\eta\} = (\eta_1, \dots, \eta_{2N})$ which consists of N out-of-plane spin deviations $(\eta_1, \dots, \eta_N) = \{m_{\vec{n}}\}$ and N canonically conjugated variables $(\eta_{N+1}, \dots, \eta_{2N}) = \{\phi_{\vec{n}}\}$ and to write the Fokker-Planck equation (16) in the form

$$\frac{\partial \mathcal{P}(\{\eta\}, t)}{\partial t} = \sum_{i,j} \frac{\partial}{\partial \eta_i} M_{i,j} \left(\frac{\partial E}{\partial \eta_j} \mathcal{P} + T \frac{\partial}{\partial \eta_j} \mathcal{P} \right) \quad (31)$$

where

$$M_{i,j} = \Gamma_i \delta_{ij} - A_{i,j} \quad (32)$$

with

$$\Gamma_i = \begin{cases} \frac{\gamma}{1-\eta_i^2}, & \text{for } i \leq N \\ \gamma(1-\eta_i^2), & \text{for } i \geq N+1 \end{cases} \quad (33)$$

and $A_{i,j}$ is the following antisymmetric matrix:

$$A_{i,j} = \begin{cases} \delta_{i+N,j}, & i \leq N \\ -\delta_{i,j+N}, & j \leq N \\ 0, & \text{otherwise} \end{cases} \quad (34)$$

$E(\{\eta\})$ is the Hamiltonian of the system expressed in terms of the variables $\{\eta\}$.

We are interested in a switching process between the vortex states with different polarization. Therefore we consider the anisotropy-temperature region (see Fig. 2) where the out-of-plane vortices are stable. In this case the energy function $E(\{\eta\})$ has a locally stable state at $\{\eta_0\}$ (an out-of-plane vortex with positive polarization) which is separated by an energy barrier from another stable state $\{-\eta_0\}$ (an out-of-plane vortex with negative polarization). We assume that the system is initially prepared in a vortex state with, say, positive polarization, and we consider the relaxation process as an escape process from the potential well which corresponds to the vortex $\{\eta_0\}$ neglecting the backward process. Another possibility to make the vortices with different polarization non-equivalent is to apply a constant magnetic field oriented along the hard-axis (perpendicular to the easy-plane). The in-plane vortex $\{\bar{\eta}\}$ with the same vorticity as the out-of-plane vortex corresponds to the energy barrier which must be overcome. The point $\{\bar{\eta}\}$ is a saddle point of $E(\{\eta\})$.

We consider a temperature which is much smaller than the energy difference between in-plane and out-of-plane vortices. After having been initially in the state $\{\eta_0\}$, the system reaches first a quasi-equilibrium state near the metastable point $\{\eta_0\}$ with the probability density \mathcal{P} given by the Gibbs distribution

$$\mathcal{P} \sim e^{-\frac{E(\{\eta\})}{T}} \quad \text{with } \{\eta\} \simeq \{\eta_0\}. \quad (35)$$

The probability flux over the barrier is concentrated in a narrow region around the saddle point $\{\bar{\eta}\}$ [29]. To obtain the flux, let D_{ni} , ($n, i = 1, \dots, 2N$) be the eigenvectors of the Hessian matrix

$$\mathcal{E}_{i,j}(\{\eta\}) = \partial^2 E / \partial \eta_i \partial \eta_j, \quad i, j = 1, \dots, 2N \quad (36)$$

evaluated at $\{\eta\} = \{\bar{\eta}\}$

$$\sum_{j=1}^{2N} \mathcal{E}_{i,j}(\{\bar{\eta}\}) D_{lj} = \mu_l D_{li} \quad (37)$$

and μ_l are the eigenvalues. Thus the energy of the system in the immediate neighborhood of the saddle point $\{\bar{\eta}\}$ can be written as

$$E = E(\{\bar{\eta}\}) + \frac{1}{2} \sum_{l=1}^{2N} \mu_l \xi_l^2 \quad (38)$$

where the new variables

$$\xi_l = \sum_{i=1}^{2N} D_{li} (\eta_i - \bar{\eta}_i) \quad (39)$$

are the principal axes coordinates.

Coming back to the original variables $m_{\bar{n}}$ and $\phi_{\bar{n}}$ we can say that the Hamiltonian of the system in the close vicinity to the in-plane vortex state can be written as

$$H = E_{\text{in-plane}} + \frac{1}{2} J \sum_{\bar{n}, \bar{\Delta}} \left(\frac{1}{2} \cos(\Phi_{\bar{n}}^0 - \Phi_{\bar{n}+\bar{\Delta}}^0) (\psi_{\bar{n}} - \psi_{\bar{n}+\bar{\Delta}})^2 + \cos(\Phi_{\bar{n}}^0 - \Phi_{\bar{n}+\bar{\Delta}}^0) m_{\bar{n}}^2 - \lambda m_{\bar{n}} m_{\bar{n}+\bar{\Delta}} \right) \quad (40)$$

where $\psi_{\vec{n}} = \Phi_{\vec{n}} - \Phi_{\vec{n}}^0$ are small deviations of the in-plane angles from their static values $\Phi_{\vec{n}}^0$. The out-of-plane spin deviations $m_{\vec{n}}$ are also assumed to be small. In this case the eigenvalues μ_l correspond to the linear spin-wave spectrum of the system in the presence of an in-plane vortex. The normal modes were investigated in [28] and it was found out that there is a particular soft mode (its frequency goes to zero for $\lambda \rightarrow \lambda_c, \lambda \leq \lambda_c$) which is responsible for the crossover from the in-plane to the out-of-plane vortex structure. In the interval $\lambda > \lambda_c$ this mode becomes unstable. In terms of Eq. (37) it means that the corresponding eigenvalue, say μ_1 , is negative.

According to [27] (see also [29]) the rate constant for an escape from the metastable point $\{\eta_0\}$ via the saddle point $\{\bar{\eta}\}$ has the form

$$\kappa = \frac{|\nu|}{2\pi} \sqrt{\frac{\det(\mathcal{E}(\{\eta_0\})/\sqrt{2\pi T})}{|\det(\mathcal{E}(\{\bar{\eta}\})/\sqrt{2\pi T})|}} \exp\left(-\frac{E(\{\bar{\eta}\}) - E(\{\eta_0\})}{T}\right) \quad (41)$$

where $|\nu|$ is the deterministic growth rate of the unstable mode at the saddle point. The quantity ν is the negative eigenvalue of the following eigenvalue problem

$$\mu_l \sum_{l'=1}^{2N} \tilde{M}_{ll'} U_{l'} = \nu U_l, \quad (42)$$

where U_l are eigenvectors and

$$\tilde{M}_{ll'} = \sum_{i,j=1}^{2N} D_{l,i} M_{i,j} D_{l',j}. \quad (43)$$

Taking into account Eq. (37) we can rewrite Eq. (43) in the form

$$\sum_{i,j=1}^{2N} \mathcal{E}_{l,j}(\{\bar{\eta}\}) M_{i,j} v_j = \nu v_i \quad (44)$$

where $v_i = \sum_{l=1}^{2N} D_{l,i} U_l$.

Coming back to the original variables $\psi_{\vec{n}}$ and $m_{\vec{n}}$ we obtain from Eqs. (32), (33), (34), (36) that the switching rate between out-of-plane vortices with opposite polarization is determined by the expression

$$\kappa = \frac{|\nu|}{2\pi} \exp\left(-\frac{F_{in} - F_{out}}{T}\right) \quad (45)$$

where

$$F_{out} = E_{out} + T \sum_m \ln(\omega_m(\text{out})/T) \quad (46)$$

is the free energy of the out-plane vortex and $\omega_m(\text{out})$ is the m -th normal mode of the vortex.

$$F_{in} = E_{in} + T \sum'_m \ln(\omega_m(\text{in})/T) + T \ln(|\omega_1(\text{in})|/T) \quad (47)$$

is an effective free energy of the in-plane vortex. In Eq. (47) the prime means the summation over the stable modes of the in-plane vortex and $|\omega_1(\text{in})|$ is the modulus of the purely imaginary frequency which corresponds to the unstable mode of the in-plane vortex.

The deterministic growth rate ν is the negative eigenvalue of the eigenvalue problem

$$\begin{aligned} \sum_{\vec{n}'} \left(\frac{\partial^2 H}{\partial \Phi_{\vec{n}} \partial \Phi_{\vec{n}'}} \right)_{m_{\vec{n}}=0, \Phi_{\vec{n}}^0} (\gamma v_{\vec{n}'}^{(1)} - v_{\vec{n}'}^{(2)}) &= \nu v_{\vec{n}}^{(1)} \\ \sum_{\vec{n}'} \left(\frac{\partial^2 H}{\partial m_{\vec{n}} \partial m_{\vec{n}'}} \right)_{m_{\vec{n}}=0, \Phi_{\vec{n}}^0} (\gamma v_{\vec{n}'}^{(2)} + v_{\vec{n}'}^{(1)}) &= \nu v_{\vec{n}}^{(2)} \end{aligned} \quad (48)$$

where $v_{\vec{n}}^{(1)}, v_{\vec{n}'}^{(2)}$ are the components of the eigenvector and we took into account that in the vicinity of the saddle point one can neglect the dependence on $m_{\vec{n}}$ in the damping constants Γ_i .

Let us evaluate these formulae in the crude approach already used in section 1. We consider the core dynamics taking into account only one pair of canonically conjugated variables m_1 and ψ_1 and putting $m_2 = m_3 = 0$, $\psi_2 = \psi_3 = 0$ in Eq. (21). In this case the eigenvalue problem (48) reduces to

$$\begin{aligned} \nu v^{(1)} - 8J\lambda_c (\gamma v^{(1)} - v^{(2)}) &= 0, \\ \nu v^{(2)} + 8J(\lambda - \lambda_c) (\gamma v^{(2)} + v^{(1)}) &= 0 \end{aligned} \quad (49)$$

where $\lambda_c = \cos \delta_1$. The deterministic growth rate ν takes on the form

$$\nu = 8J \left((\lambda_c - \frac{\lambda}{2})\gamma - \frac{1}{2}\sqrt{\lambda^2\gamma^2 + 4(\lambda - \lambda_c)\lambda_c} \right). \quad (50)$$

The out-of-plane vortex exists for $\lambda > \lambda_c$ and the static value of the out-of-plane spin deviation is $m_1^0 = \pm \sqrt{1 - \frac{\lambda_c^2}{\lambda^2}}$. The Hessian matrix (36) is evaluated at the metastable point (out-of-plane vortex) and at the saddle point (in-plane vortex) which yields

$$4J \begin{pmatrix} \frac{\lambda(\lambda^2 - \lambda_c^2)}{\lambda_c^2} & 0 \\ 0 & \frac{\lambda_c^2}{\lambda} \end{pmatrix}, \quad 4J \begin{pmatrix} -(\lambda - \lambda_c) & 0 \\ 0 & \lambda_c \end{pmatrix} \quad (51)$$

respectively. Inserting Eqs. (50), (51) into (41) yields

$$\kappa = 2J \frac{\sqrt{\lambda^2\gamma^2 + 4\lambda_c(\lambda - \lambda_c)} + \gamma(\lambda - 2\lambda_c)}{\pi} \sqrt{\frac{\lambda + \lambda_c}{\lambda_c}} e^{-\frac{E_{in} - E_{out}}{T}} \quad (52)$$

We see that in the low-damping limit the switching rate reduces to

$$\kappa = \frac{2J}{\pi} \sqrt{\lambda^2 - \lambda_c^2} e^{-\frac{E_{in} - E_{out}}{T}} \quad (53)$$

while in the overdamped limit

$$\kappa = \frac{2J\gamma}{\pi} (\lambda - \lambda_c) \sqrt{\frac{\lambda + \lambda_c}{\lambda_c}} e^{-\frac{E_{in} - E_{out}}{T}}. \quad (54)$$

We note that the expressions (52), (53) and (54) are valid only when $\frac{E_{in} - E_{out}}{T} \gg 1$. This condition is not fulfilled when $\lambda \rightarrow \lambda_c$.

IV. LANGEVIN DYNAMICS SIMULATIONS

In order to test our theory we have numerically integrated the stochastic Landau-Lifshitz equation (2) for a large square lattice in which we cut out a circle with radius L using free boundary conditions. As initial spin configuration we take an out-of-plane vortex with center at a distance R_0 from the middle of the circle. Since the anisotropy parameter λ should not be chosen close to λ_c (see section II), the diameter $2r_v$ of the out-of-plane vortex structure in any case is considerably larger than the lattice constant. This has the advantage that the vortex can move smoothly over the Peierls-Navarro potential of the lattice; indeed discreteness effects are hardly visible in the motion.

Without noise and damping the trajectory $\vec{X}(t)$ of the vortex center would be a circle with radius R_0 in a first approximation which is given by the Thiele equation [20]

$$\vec{G} \times \dot{\vec{X}} = \vec{F}. \quad (55)$$

The driving force \vec{F} is the 2D Coulomb force between the vortex and an image vortex which is located at the distance L^2/R_0 from the circle center [23]. The image has opposite vorticity but the same polarization as the vortex (for free boundary conditions). Eq. (55) was derived from the Landau-Lifshitz equation in the continuum limit, assuming a rigid vortex shape. In a better approximation the trajectories turn out to be a superposition of cycloids around the circular motion [32], but this fact seems to be unimportant for the switching process which we discuss here.

When the damping term in (2) is included, the vortex moves outwards on a spiral [33], until it finally reaches the boundary where an annihilation together with the image takes place. However, we choose an initial position far away from the boundary and a very small damping parameter; therefore we have plenty of time to observe the motion of the vortex before it gets close to the boundary.

When the stochastic fields $\vec{h}_{\vec{n}}(t)$ in (2) are included, the vortex trajectories naturally become noisy. In this case the variances $\langle X_i^2 \rangle - \langle X_i \rangle^2$ can be computed as a function of time and can be compared with a collective variable theory for finite temperature [34], [35], [36]. This yields an effective vortex diffusion constant D_v .

In contrast to the vorticity q , the polarization p of the vortex is not a constant of motion in a discrete system: The out-of-plane vortex structure can flip to the other polarization due to the stochastic fields. Then the direction of $\vec{G} = 2\pi qp\vec{e}_z$ is reversed and thus the direction of the vortex motion is reversed, too, as can be seen from (55).

In order to measure the transition rate κ in the simulations it is necessary to choose carefully the parameter ranges: λ has already been discussed above, we take $\lambda = 0.9$ which is sufficiently far away from both $\lambda_c \simeq 0.70$ and the isotropic limit $\lambda = 1$. For our circular system we choose a radius $L = 24$ which provides enough space for the vortex (the out-of-plane vortex structure should not contact the boundary even during long integration times). For the same reason the initial distance R_0 of the vortex center from the middle of the circle should not be too large. On the other hand R_0 should not be too small, otherwise the driving force \vec{F} would not be strong enough to overcome the pinning forces of the lattice. Choosing $R_0 \simeq 10$ both conditions can be fulfilled, if the damping γ is small enough. (The larger γ is, the sooner the vortex reaches the boundary). On the other hand, a small γ means a long saturation time (after the start of the simulation the energy rises and saturates at a value independent of γ). For $\gamma \geq 0.002$ we get acceptable saturation times < 300 (in units of $\hbar/(JS)$).

The most important parameter naturally is the temperature: For $T \ll E_{in} - E_{out}$ the transition rate κ in (52) is extremely small and thus the integration times would be much too long, which are needed to get a sufficient number of transition events.

On the other hand T should not be too large, otherwise vortex-antivortex pairs appear spontaneously in the vicinity of the vortex. This definitely changes the translational motion of the vortex, and it is possible that the transition to the other polarization is influenced, too. The difference $E_{in} - E_{out}$ can be estimated by comparing the total energies of our system with $L = 24$ in the presence of a static in-plane or out-of-plane vortex at the center of a lattice cell: $E_{in} - E_{out} = 109.40 - 108.49 = 0.91$ (in units of J). The factor in front of the exponential in Eq. (53) is approximately 0.12 therefore $0.1 \leq T \leq 0.3$ is expected to be an appropriate temperature range (The Kosterlitz-Thouless transition temperature is about 0.8 for $\lambda = 0$).

The initial spin configuration for our simulations stems from an iterative program [24] which produces a discrete vortex structure on the lattice (In this way we avoid the radiation of spin waves which would occur during the first time units if a continuum approach for the vortex structure were used). As we interpret the Landau-Lifshitz Eq. (2) as a Stratonovich stochastic equation and as we use multiplicative noise, we take the Heun integration scheme which was developed for this situation [37], [38]. The spin length S is conserved in Eq. (2) and can be used as a test of the program, the time step is 0.01, in units of $\hbar/(JS)$.

For reasons to discuss below, we have performed two different types of simulations: In type I a complete simulation for one temperature consists of many runs with different sequences of random numbers which produce the white noise. The total integration time is divided into a first part of length t_0 (denoted as pre-run) and a second part of length t (denoted as main run). We choose t_0 in the order of 1000 which is larger than the saturation time and large enough that the vortex has no memory of the configuration from which it started; i. e. in every run we have at the time t_0 a different initial condition for the main run. Only the main runs are used for the thermal average: the average time τ , after which the *first* transition of the vortex to the opposite polarization occurs, is obtained from

$$N(t) = N_0 e^{-t/\tau}. \quad (56)$$

Here N_0 and N are the number of runs in which the vortex has made no transition until t_0 and $t_0 + t$, respectively. τ must be compared with the inverse transition rate $\kappa^{-1} = \tau_{th}$ from Eq. (53), because we work with a small damping parameter $\gamma = 0.002$ (Table I). The agreement is rather good, taking into account that we used a very crude model for the vortex core formed from only the four innermost spins.

We counted only the first transitions because in our theory we have calculated the escape rate from a metastable state. After the first transition the vortex is typically in a different dynamical state than before, thus the probability for the next transition is expected to be different, too. In fact, we obtained a total number of 870 transitions in 158 runs with $t = 4000$ for $T = 0.15$; this means that the average transition time is 917, which is about four times smaller than the first-transition time 4286 in Table I.

In a type-II simulation we only make one pre-run of length t_0 , i. e. the main runs all start from the same initial condition. By taking different lengths t_0 we can see whether τ depends on t_0 and/or the initial condition. We performed this type of simulations because we had some hints from the investigation of the variances [35] that a

certain vortex mode might be gradually excited thermally which could trigger the transition. The frequency of this mode is very low, namely $\Delta\omega = \omega_1 - \omega_2$, where $\omega_{1,2}$ are the eigenfrequencies of two quasi-local modes of the circular system with one vortex [39]. $\omega_{1,2}$ are identical to the frequencies of the cycloidal oscillations of the vortex trajectory around the mean path (see above).

However, our type-II simulations in Table I do not reveal a correlation between the length t_0 of the pre-run and the first transition time τ . Nevertheless the values of τ differ considerably for the different simulations. Thus we conclude that τ depends strongly on the initial condition, which is identical for all main runs of one simulation. This conclusion is confirmed by looking at the first 200 time units immediately after the beginning of the main runs: E. g., in simulation No. 7 about 20% of the vortices switched over to the other polarization, while in No. 6 no vortex did so (Fig. 3). A closer inspection of the initial spin configurations shows that τ depends both on the position of the vortex center within a lattice cell and on the dynamical state of the vortex.

An additional test of the above conclusion was made by leaving out the first 500 time units of each main run (dash-dotted line in Fig. 3). Then we expect that the vortices have no memory of their initial condition and the resulting τ should be the same as in the type-I simulations (within the statistical errors). In fact, this is confirmed by comparing No. 8 with No. 2 in Table I.

V. CONCLUSION

In this work we used a very simplified Hamiltonian for the cores of both planar and nonplanar vortices. Adding white noise to the local fields in which the classical spins precess we obtained a Landau-Lifshitz equation with multiplicative stochastic forces. The stationary solution of the corresponding Fokker-Planck equation exhibits two maxima for the two possible polarizations of the nonplanar vortex and a saddle point for the planar vortex, if the anisotropy parameter lies in a certain, temperature-dependent range.

We calculated the rate κ for the transition from one polarization to the opposite one. Our results were tested by long-time Langevin dynamics simulations of the full many-spin model at three temperatures well below the Kosterlitz-Thouless phase transition temperature. The agreement is rather good, considering that the vortex core was described only approximately by using only the four innermost spins. We did not make any tests for higher temperatures because the probability for the spontaneous appearance of a vortex-antivortex pair in the vicinity becomes too large; the interaction with this pair could then influence κ .

We emphasize that the above results were obtained by effectively averaging over many initial conditions. This is necessary because our simulations demonstrate that the transition rate depends very strongly on the initial condition, i. e. both on the position of the vortex center within a lattice cell and on the velocity of the vortex at this position.

VI. ACKNOWLEDGEMENTS

Yu. Gaididei would like to express his thanks for the hospitality of the University of Bayreuth where this work was done. Partial support was received from project No. X 271.5 of the scientific and technological cooperation between Germany and Ukraine. Work at Los Alamos National Laboratory is supported by the USDoE.

-
- [1] L. J. de Jongh, *Magnetic Properties of Layered Transition Metal Compounds* (Kluwer Academic Publisher, 1990)
 - [2] L. P. Regnault, C. Lartigue, J. F. Legrand, B. Farago, J. Rossat-Mignot, J. Y. Henry, *Physica D* **B156-157**, 298 (1989)
 - [3] P. Gaveau, J. P. Boucher, L. P. Regnault, J. Y. Henry, *J. Appl. Phys.* **69**(27), 6228 (1991)
 - [4] K. Hirakawa, H. Yoshizawa, K. Ubokoshi, *J. Phys. Soc. Japan* **51**, 2151 (1982)
 - [5] D. G. Wiesler, H. Zabel, S. M. Shapiro, *Physica* **B156-157**, 292 (1989)
 - [6] M. Pomerantz, *Surf. Sci.* **142**, 556 (1984); D. I. Head, B. H. Blott, and D. Melville, *J. Phys. (Paris) Colloq.* **49**, C8-1649 (1988)
 - [7] S. Iida, *J. Phys. Chem. Solids* **24**, 625 (1963).
 - [8] C. W. Gardiner, *Handbook of Stochastic Methods*, (Springer-Verlag, New York, Heidelberg, Berlin, 1983).
 - [9] M. T. Hutchings, P. Day, E. Janke, and R. Pynn, *J. Magn. Mater.* **54-57**, 673, (1986)
 - [10] L. R. Regnault, J. P. Boucher, J. Rossat-Mignod, J. Bouillot, R. Pynn, J. Y. Henry, and J. P. Renard, *Physica B+C* **136B**, 329 (1986)

- [11] L. P. Regnault and J. Rossat-Mignod, in *Magnetic Properties of Layered Transition Metal Compounds*, ed. by L. J. de Jongh and R. D. Willet (Reidel, Dordrecht, 1987)
- [12] S. T. Bramwell, M. T. Hutchings, J. Norman, R. P. Pynn, and P. Day, *J. de Physique*, Colloque C8, 1435 (1988)
- [13] D. G. Wiesler, H. Zabel, and S. M. Shapiro, *Z. Phys. B* **93**, 277 (1994)
- [14] F. G. Mertens, A. R. Bishop, G. M. Wysin, and C. Kawabata, *Phys. Rev. Lett.* **59**, 117 (1987)
- [15] F. G. Mertens, A. R. Bishop, G. M. Wysin, and C. Kawabata, *Phys. Rev. B* **39**, 591 (1989)
- [16] M. E. Gouvea, G. M. Wysin, A. R. Bishop, and F. G. Mertens, *Phys. Rev. B* **39**, 11840 (1989)
- [17] A. R. Völkel, G. M. Wysin, A. R. Bishop, and F. G. Mertens, *Phys. Rev. B* **44**, 10066 (1991)
- [18] A. R. Völkel, A. R. Bishop, F. G. Mertens, and G. M. Wysin, *J. Phys.: Cond. Matter* **4**, 9411 (1992)
- [19] A. R. Völkel, F. G. Mertens, A. R. Bishop, and G. M. Wysin, *Ann. Phys. (Weinheim, Germany)* **2**, 308 (1993)
- [20] A. A. Thiele, *Phys. Rev. Lett.* **30**, 230 (1973).
- [21] D. L. Huber, *Phys. Rev. B* **26**, 3758 (1982).
- [22] A. R. Völkel, F. G. Mertens, A. R. Bishop, and G. M. Wysin, *Phys. Rev.* **B43**, 5992 (1991)
- [23] F. G. Mertens, G. M. Wysin, A. R. Völkel and A. R. Bishop, *Cyclotron-Like Oscillations and Boundary Effects in the 2-Vortex Dynamics of Easy-Plane Magnets*, in *Nonlinear coherent structures in physics and biology*, ed. by K. H. Spatschek and F. G. Mertens (NATO ASI Series, Vol. B 329, Plenum Press, New York, 1994).
- [24] H.-J. Schnitzer, *Zur Dynamik kollektiver Anregungen in Hamiltonschen Systemen*, Ph.D.-thesis, University of Bayreuth (1996).
- [25] G. M. Wysin, *Phys. Rev. B* **49**, 8780 (1994).
- [26] G. M. Wysin, *Phys. Lett. A* **240**, 95 May 14. (1998).
- [27] J. S. Langer, *Ann. Phys. N. Y.*, **54**, 258 (1969).
- [28] G. M. Wysin, A. R. Völkel, *Phys. Rev. B* **52**, 7412 (1995).
- [29] P. Hänggi, P. Talkner, and M. Borkovec, *Rev. Mod. Phys.* **62**, 251 (1990).
- [30] *Higher Transcendental Functions* Vol. II (McGraw-Hill Book Company, Inc., 1953).
- [31] M. Abramowitz and I. Stegun, *Handbook of Mathematical Functions* (Dover Publications, Inc., New York, 1972).
- [32] F. G. Mertens, H. J. Schnitzer, A. R. Bishop, *Phys. Rev. B* **56**, 5 (1997).
- [33] A. R. Voelkel, G. M. Wysin, F. G. Mertens, A. R. Bishop, H. J. Schnitzer, *Phys. Rev. B* **44**, 10066 (1991).
- [34] T. Kamppeter, F. G. Mertens, A. Sánchez, N. Grønbech-Jensen, A. R. Bishop, F. Domínguez-Adame, *Dynamics of Nonplanar Vortices in the Classical 2D Anisotropic Heisenberg Model at Finite Temperatures*, contribution for the 165th Heraeus Seminar held at Bad Honnef, October 14-16, 1996, in *Theory of Spin Lattices and Lattice Gauge Models*, ed. by M. L. Ristig, K. A. Gernoth, J. W. Clark, *Lecture notes in physics*, Vol. 494 (Springer, Berlin, 1997).
- [35] T. Kamppeter, F. G. Mertens, A. Sánchez, F. Domínguez-Adame, A. R. Bishop, N. Grønbech-Jensen, *Temperature Effects on Vortex Dynamics of the Two Dimensional Anisotropic Heisenberg Model*, in *Proceedings of the VIII Spanish Meeting on Statistical Physics FISES '97*, ed. by J. A. Cuesta and A. Sánchez (Editorial del CIEMAT, Madrid, 1998).
- [36] T. Kamppeter, F. G. Mertens, A. Sánchez, A. R. Bishop, F. Domínguez-Adame, and N. Grønbech-Jensen, *Eur. Phys. J. B*, in press.
- [37] T. C. Gard, *Introduction to Stochastic Differential Equations*, Marcel Dekker, vol. 114 of *Monographs and Textbooks in Pure and Applied Mathematics* (1987).
- [38] M. San Miguel, R. Toral, *Stochastic Effects in Physical Systems in Instabilities and Nonequilibrium Structures VI*, Ed. E. Tirapegui, Kluwer Academic (1998).
- [39] B. A. Ivanov, H. J. Schnitzer, F. G. Mertens, G. M. Wysin, *Magnon Modes and Magnon-Vortex Scattering in 2D Easy-Plane Ferromagnets*, *Phys. Rev. B* **58**, 8464 (1998).

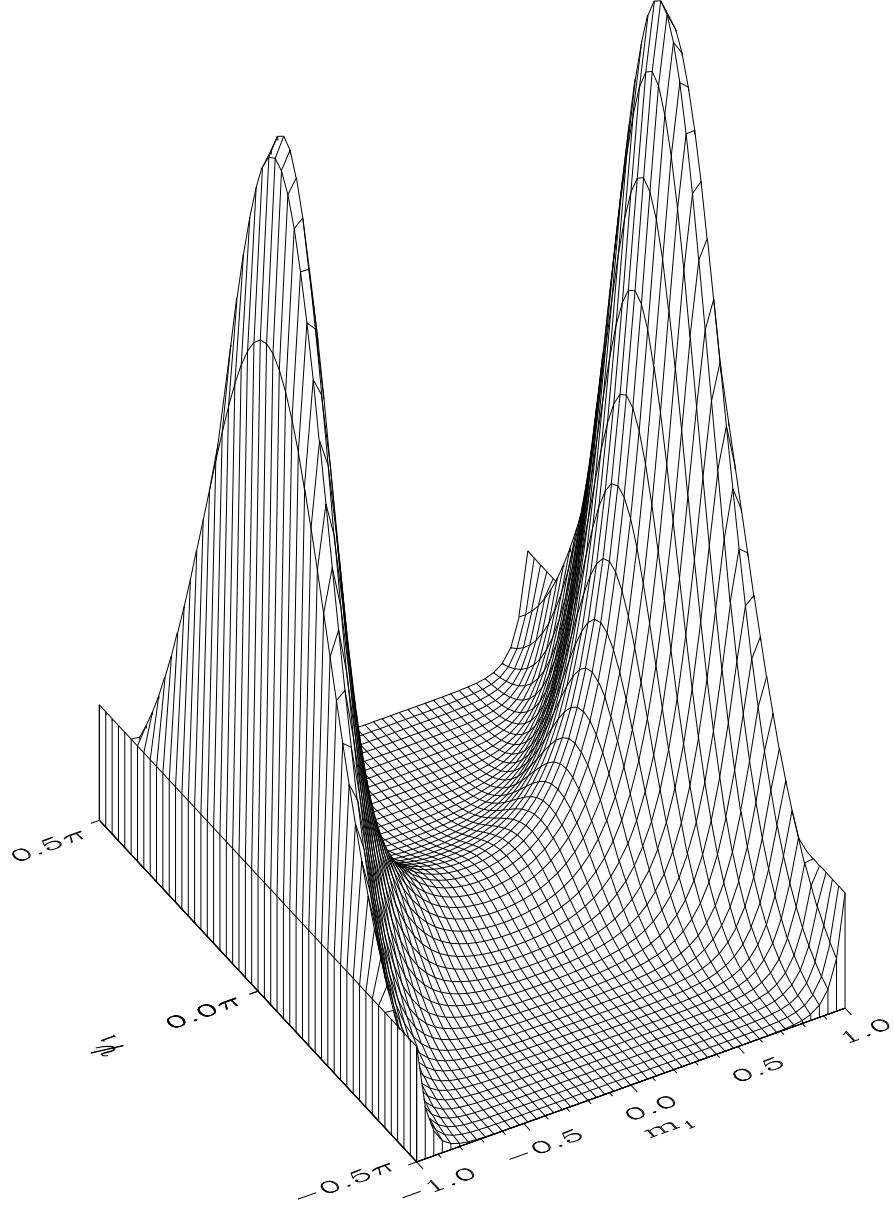
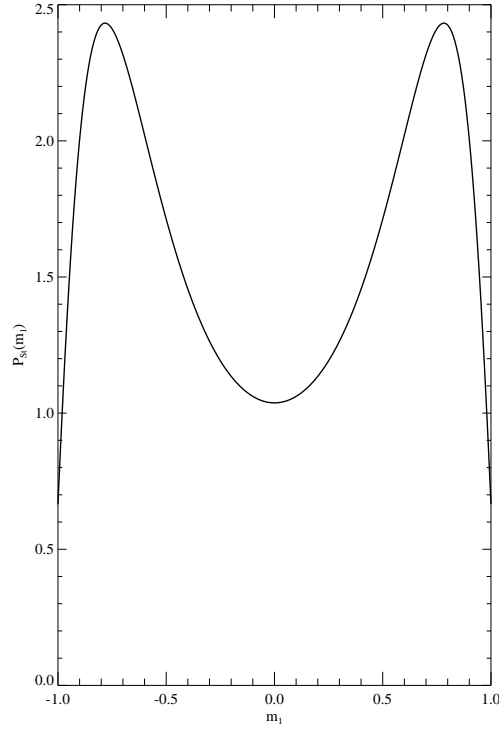


Fig. 1. (a) Stationary probability distribution (14) (without normalization), using the simplified core Hamiltonian (26). m_1 and ψ_1 are the deviations (20) and (19) of the out-of-plane components and in-plane angles from their static values, resp..



(b) Reduced stationary distribution (27), obtained by integrating the distribution in (a) over ψ_1 .

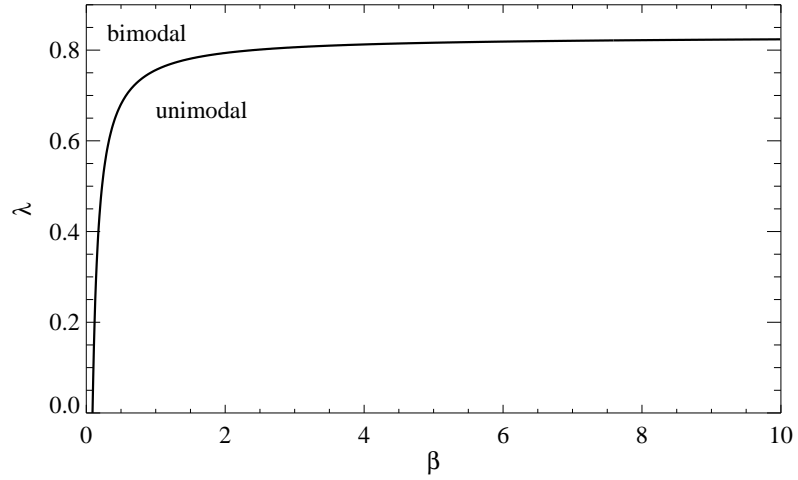


Fig. 2. λ vs. β phase diagram. Above the bifurcation curve $\lambda(\beta)$ there are two maxima in \mathcal{P}_{st} , corresponding to the two polarizations of a nonplanar vortex, and one saddle point corresponding to a planar vortex structure.

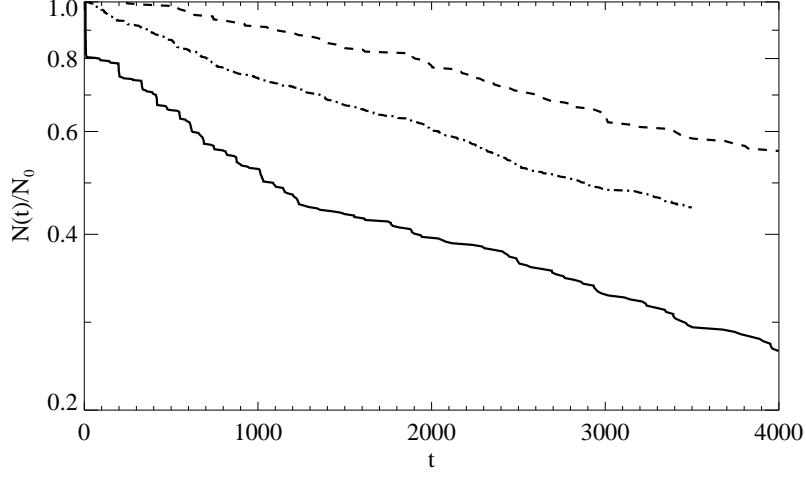


Fig. 3. Percentage of vortices which have not yet made a transition to the opposite polarization up to the time t of a type-II simulation. The temperature is $T = 0.15$. The solid and dashed lines represent two sets of runs (No. 7 and 6 in Table I) with different initial configurations (which arise from using two different lengths t_0 for the pre-run). The dash-dotted line results from sampling the transition times from the simulations No. 4 - 7 of Table I, omitting the first 500 time units of each main run.

TABLE I. Transition times τ from simulations, with statistical errors τ_{rms}/τ , compared to the theoretical estimates τ_{th}

No.	type	T	t_0	t	N_0	N	τ	τ_{rms}/τ	τ_{th}
1	I	0.1	1200	3800	497	477	92516	22%	70334
2	I	0.15	1200	3800	407	158	4016	6%	3386
3	I	0.2	1200	3800	100	1	825	10%	743
4	II	0.15	1200	4000	254	100	4291	8%	—
5	II	0.15	2200	4000	264	100	4120	8%	—
6	II	0.15	3200	4000	181	100	6741	11%	—
7	II	0.15	4200	4000	405	100	2859	6%	—
8	II	0.15	—	3500	905	400	4286	5%	3386